J|A|C|S
ARTICLES
Published on Web 11/16/2002

Electrical Contacting of Flavoenzymes and NAD(P)$^+$-Dependent Enzymes by Reconstitution and Affinity Interactions on Phenylboronic Acid Monolayers Associated with Au-Electrodes

Maya Zayats, Eugenii Katz, and Itamar Willner*

Contribution from the Institute of Chemistry, The Hebrew University of Jerusalem, Jerusalem 91904, Israel

Received July 30, 2002

Abstract: The preparation of integrated, electrically contacted, flavoenzyme and NAD(P)$^+$-dependent enzyme-electrodes is described. The reconstitution of apo-glucose oxidase, apo-GOx, on a FAD cofactor linked to a pyrroloquinoline quinone (PQQ) phenylboronic acid monolayer yields an electrically contacted enzyme monolayer (surface coverage 2.1×10^{-12} mol cm^{-2}) exhibiting a turnover rate of 700 s^{-1} (at 22 ± 2 °C). The system is characterized by microgravimetric quartz-crystal microbalance analyses, Faradaic impedance spectroscopy, rotating disk electrode experiments, and cyclic voltammetry. The performance of the enzyme-electrode for glucose sensing is described. Similarly, the electrically contacted enzyme-electrodes of NAD(P)$^+$-dependent enzymes malate dehydrogenase, MalD, and lactate dehydrogenase, LDH, are prepared by the cross-linking of affinity complexes generated between the enzymes and the NADP$^+$ and NAD$^+$ cofactors linked to a pyrroloquinoline quinone phenylboronic acid monolayer, respectively. The MalD enzyme-electrode (surface coverage 1.2×10^{-12} mol cm^{-2}) exhibits a turnover rate of 190 s^{-1}, whereas the LDH enzyme-electrode (surface coverage 7.0×10^{-12} mol cm^{-2}) reveals a turnover rate of 2.5 s^{-1}. Chronoamperometric experiments reveal that the NAD$^+$ cofactor is linked to the PQQ-phenylboronic acid by two different binding modes. The integration of the LDH with the two NAD$^+$ cofactor configurations yields enzyme assemblies differing by 1 order of magnitude in their bioelectrocatalytic activities.

Introduction

Electrical contacting of redox-enzymes with electrodes is a key process in the tailoring of enzyme-electrodes for bioelectronic applications such as biosensors[1] or biofuel cell elements.[2] While redox-enzymes usually lack direct electrical communication with electrodes, the application of diffusional electron mediators,[3] the tethering of redox-relay groups to the protein,[4] or the immobilization of the enzymes in redox-active polymers[5] was widely applied to establish electrical communication between the redox-proteins and the electrodes. Nonetheless, relatively inefficient electrical contacting of the enzymes with the electrode is achieved due to the nonoptimal modification of the enzymes by the redox-tethers,[6] or the lack of inappropriate alignment of the enzymes with respect to the electrode. Very efficient electrical communication between redox-proteins and electrodes was achieved by the reconstitution of apo-enzymes on relay-cofactor monolayers associated with electrodes.[7−9] For example, apo-glucose oxidase was reconstituted on a relay-FAD monolayer,[7] and apo-glucose dehydrogenase was reconstituted on a pyrroloquinoline quinone (PQQ)-modified polyaniline film associated with an electrode.[9] These procedures for the electrical contacting of redox-enzymes with electrodes may be applied on proteins that include an embedded redox center such as flavoenzymes,[7] hemoproteins,[8] or pyrroloquinoline quinone

* To whom correspondence should be addressed. Tel.: 972-2-6585272. Fax: 972-2-6527715. E-mail: willnea@vms.huji.ac.il.

(1) (a) Armstrong, F. A.; Wilson, G. S. *Electrochim. Acta* **2000**, *45*, 2623−2645. (b) Willner, I.; Katz, E. *Angew. Chem., Int. Ed.* **2000**, *39*, 1180−1218. (c) Habermuller, L.; Mosbach, M.; Schuhmann, W. *Fresenius' J. Anal. Chem.* **2000**, *366*, 560−568. (d) Willner, I.; Willner, B. *Trends Biotechnol.* **2001**, *19*, 222−230. (e) Armstrong, F. A.; Heering, H. A.; Hirst, J. *Chem. Soc. Rev.* **1997**, *26*, 169−179.

(2) (a) Willner, I.; Katz, E.; Patolsky, F.; Bückmann, A. F. *J. Chem. Soc., Perkin Trans. 2* **1998**, 1817−1822. (b) Katz, E.; Willner, I.; Kotlyar, A. B. *J. Electroanal. Chem.* **1999**, *479*, 64−68. (c) Katz, E.; Shipway, A. N.; Willner, I. In *Handbook of Fuel Cell Technology*; Vielstich, Gasteiger, H., Eds.; Wiley: New York, 2002; in press. (d) Tsujimura, S.; Fujita, M.; Tatsumi, H.; Kano, K.; Ikeda, T. *Phys. Chem. Chem. Phys.* **2001**, *3*, 1331−1335. (e) Chen, T.; Barton, S. C.; Binyamin, G.; Gao, Z. Q.; Zhang, Y. C.; Kim, H. H.; Heller, A. *J. Am. Chem. Soc.* **2001**, *123*, 8630−8631. (f) Katz, E.; Bückmann, A. F.; Willner, I. *J. Am. Chem. Soc.* **2001**, *123*, 10752−10753.

(3) Bartlett, P. N.; Tebbutt, P.; Whitaker, R. G. *Prog. React. Kinet.* **1991**, *16*, 55−155.

(4) (a) Degani, Y.; Heller, A. *J. Phys. Chem.* **1987**, *91*, 1285−1289. (b) Degani, Y.; Heller, A. *J. Am. Chem. Soc.* **1988**, *110*, 2615−2620. (c) Schuhmann, W.; Ohara, T. J.; Schmidt, H.-L.; Heller, A. *J. Am. Chem. Soc.* **1991**, *113*, 1394−1397. (d) Willner, I.; Katz, E.; Riklin, A.; Kasher, R. *J. Am. Chem. Soc.* **1992**, *114*, 10965−10966. (e) Willner, I.; Riklin, A.; Shoham, B.; Rivenzon, D.; Katz, E. *Adv. Mater.* **1993**, *5*, 912−915.

(5) (a) Emr, S. A.; Yacynych, A. M. *Electroanalysis* **1995**, *7*, 913−923. (b) Heller, A. *Acc. Chem. Res.* **1990**, *23*, 128−134.

(6) Badia, A.; Carlini, R.; Fernandez, A.; Battaglini, F.; Mikkelsen, S. R.; English, A. M. *J. Am. Chem. Soc.* **1993**, *115*, 7053−7060.

(7) (a) Willner, I.; Heleg-Shabtai, V.; Blonder, R.; Katz, E.; Tao, G.; Bückmann, A. F.; Heller, A. *J. Am. Chem. Soc.* **1996**, *118*, 10321−10322. (b) Katz, E.; Riklin, A.; Heleg-Shabtai, V.; Willner, I.; Bückmann, A. F. *Anal. Chim. Acta* **1999**, *385*, 45−58. (c) Raitman, O. A.; Katz, E.; Bückmann, A. F.; Willner, I. *J. Am. Chem. Soc.* **2002**, *124*, 6487−6496.

(8) (a) Zimmermann, H.; Lindgren, A.; Schuhmann, W.; Gorton, L. *Chem.-Eur. J.* **2000**, *6*, 592−599. (b) Guo, L.-H.; McLendon, G.; Razafitrimo, H.; Gao, Y. *J. Mater. Chem.* **1996**, *6*, 369−374.

(9) Raitman, O. A.; Patolsky, F.; Katz, E.; Willner, I. *Chem. Commun.* **2002**, 1936−1937.

10.1021/ja027919y CCC: $22.00

(PQQ)-containing enzymes.[9] The vast majority of redox-enzymes are, however, NAD(P)$^+$/NAD(P)H-dependent biocatalysts, and their electrical contacting reveals fundamental difficulties due to the diffusional nature of the operation of these cofactors. That is, the biocatalytic activity of these enzymes involves the diffusion of the NAD(P)$^+$/NAD(P)H cofactors into the proteins, the formation of temporary complexes that enable electron (hydride) transfer between the redox center and the cofactor, and the subsequent diffusion of the reduced (or oxidized) cofactor from the protein matrixes.[3] For the design of enzyme-electrodes for bioelectronic applications, however, it is essential to generate integrated biomaterial-electrodes that lack diffusional components. A further difficulty accompanying NAD(P)$^+$/NAD(P)H-dependent enzymes relates to the poor electrochemical properties of the NAD(P)$^+$/NAD(P)H cofactors. The direct electrochemical oxidation of NAD(P)H or the direct reduction of NAD(P)$^+$ is kinetically unfavored leading to high overpotentials[10] that structurally change the respective cofactors and inhibit their biological function.[11] Different redox-mediators were employed for the catalyzed oxidation of NAD(P)H.[12−14] Electroactive relays, such as *o*-quinones, *p*-quinones, phenazine, phenoxazine, and phenothiazine derivatives, ferrocenes, and Os-complexes, were used as catalysts for the oxidation of NAD(P)H. A particularly effective catalyst for the electro-oxidation of NAD(P)H is pyrroloquinoline quinone (PQQ).[15,16] The enhanced electrocatalyzed oxidation of NAD(P)H in the presence of Ca^{2+}-ion was reported,[15] and the electrocatalytic regeneration of NADP$^+$ in a PQQ-malic enzyme monolayer assembly was achieved.[16] Similarly, electrocatalyzed reduction of NAD(P)$^+$ was accomplished in the presence of Rh-complexes.[17]

Modified NAD$^+$ derivatives were linked to polymer matrixes[18] and coupled to NAD$^+$-dependent enzymes.[19] The coimmobilization of the polymer-bound cofactors and biocatalysts led to the design of bioreactors for biocatalytic transformations[20] and to the organization of biosensor devices.[21] An integrated NAD$^+$-dependent enzyme-electrode was generated by the two-dimensional cross-linking of an affinity complex generated between a PQQ-NAD$^+$ monolayer and the respective cofactor-dependent enzyme, for example, lactate dehydrogenase.[22] Nonetheless, the generation of the electrically contacted flavoenzyme-electrode, or of the NAD$^+$-dependent enzyme-electrode, required the use of the scarce amino-functionalized FAD and NAD$^+$ cofactors,[23] respectively. This turned the reconstitution of the enzymes or the lateral cross-linking of the NAD$^+$-enzyme complexes to yield electrically contacted enzyme-electrodes to be of limited applicability.

Recently, we reported in a preliminary communication on the use of a boronic acid-functionalized relay monolayer as an active interface for the ligation of native flavin adenine dinucleotide, FAD, and for the surface reconstitution of the flavo-apoenzyme glucose oxidase on the monolayer to yield an electrically contacted enzyme-electrode.[24] Here we wish to present the detailed comprehensive study characterizing the generation of integrated electrically contacted enzyme-electrodes of the flavoenzyme glucose oxidase, the NAD$^+$-dependent enzyme lactate dehydrogenase, and the NADP$^+$-dependent biocatalyst malate dehydrogenase by the ligation of the native FAD, NAD$^+$, and NADP$^+$ cofactors to a relay boronic-acid monolayer associated with a Au-electrode. The surface-reconstitution of the apo-glucose oxidase on the FAD monolayer, or the two-dimensional cross-linking of the complexes generated by the NAD$^+$ or NADP$^+$ monolayers with the respective enzyme, led to the electrically contacted enzyme-electrodes.

Experimental Section

Chemicals. Lactate dehydrogenase (LDH, EC 1.1.1.27 from rabbit muscle, type II), malate dehydrogenase (MalD, EC 1.1.1.40 from chicken liver), and glucose oxidase (GOx, EC 1.1.3.4 from *Aspergillus niger*) were purchased from Sigma and used without further purification. Apo-glucose oxidase (apo-GOx) was prepared by a modification[7b] of the reported method.[25] The cofactors of LDH, MalD, and GOx − β-nicotinamide adenine dinucleotide (NAD$^+$), β-nicotinamide adenine dinucleotide phosphate (NADP$^+$), and flavin adenine dinucleotide (FAD), respectively − were purchased from Sigma and used without further purification. All other chemicals, including pyrroloquinoline quinone (PQQ), 3-aminophenylboronic acid, 2,2′-dithio-bis(ethaneamine) (cystamine), dithiobis(succinimidylpropionate), 1-tetradecanethiol, 4-(2-hydroxyethyl)piperazine-1-ethanesulfonic acid sodium salt (HEPES), tris(hydroxymethyl)aminomethane hydrochloride (Tris), 1-ethyl-3-(3-dimethylaminopropyl)carbodiimide (EDC), glutaric dialdehyde, β-D-(+)-glucose, lactic acid, L-malic acid, and ferrocene monocarboxylic acid, were purchased from Sigma and Aldrich and used as supplied. Ultrapure water from Seralpur Pro 90 CN source was used in all experiments.

Modification of Electrodes. Au-electrodes (0.5 mm diameter Au wire, geometrical area ca. 0.29 cm^2, roughness factor ca. 1.4) were used for modifications. The Au-electrodes were cleaned by boiling in 2 M KOH for 1 h followed by rinsing with water. The electrodes were

(10) (a) Blaedel, W. J.; Jenkins, R. A. *Anal. Chem.* **1975**, *47*, 1337−1343. (b) Samec, Z.; Elving, P. J. *J. Electroanal. Chem.* **1983**, *144*, 217−234. (c) Burnett, J. N.; Underwood, A. L. *Biochemistry* **1975**, *5*, 2060−2066. (d) Schmakel, C. O.; Santhanam, K. S. V.; Elving, P. J. *J. Am. Chem. Soc.* **1975**, *97*, 5083−5092.
(11) Cunningham, A. J.; Underwood, A. L. *Biochemistry* **1976**, *6*, 266−271.
(12) (a) Katakis, I.; Dominguez, E. *Mikrochim. Acta* **1997**, *126*, 11−32. (b) Gorton, L.; Persson, B.; Hale, P. D.; Boguslavsky, L. I.; Karan, H. I.; Lee, H. S.; Skotheim, T. A.; Lan, H. L.; Okamoto, Y. In *Biosensors and Chemical Sensors*; Edelman, P. G., Wang, J., Eds.; American Chemical Society: Washington, D.C., 1992; Chapter 6, pp 56−83.
(13) (a) Jaegfeldt, H.; Kuwana, T.; Johansson, G. *J. Am. Chem. Soc.* **1983**, *105*, 1805−1814. (b) Miller, L. L.; Valentine, J. R. *J. Am. Chem. Soc.* **1988**, *110*, 3982−3989.
(14) (a) Gorton, L. *J. Chem. Soc., Faraday Trans. 1* **1986**, *82*, 1245−1258. (b) Persson, B.; Gorton, L. *J. Electroanal. Chem.* **1990**, *292*, 115−138. (c) Schlereth, D. D.; Katz, E.; Schmidt, H.-L. *Electroanalysis* **1995**, *7*, 46−54.
(15) Katz, E.; Lötzbeyer, T.; Schlereth, D. D.; Schuhmann, W.; Schmidt, H.-L. *J. Electroanal. Chem.* **1994**, *373*, 189−200.
(16) Willner, I.; Riklin, A. *Anal. Chem.* **1994**, *66*, 1535−1539.
(17) (a) Ruppert, R.; Hermann, S.; Steckhan, E. *Tetrahedron Lett.* **1987**, *28*, 6583−6586. (b) Wienkamp, R.; Steckhan, E. *Angew. Chem., Int. Ed. Engl.* **1982**, *21*, 782−783. (c) Chardonnoblat, S.; Cosnier, S.; Deronzier, A.; Vlachopoulos, N. *J. Electroanal. Chem.* **1993**, *352*, 213−228.
(18) (a) Schmidt, H.-L.; Grenner, G. *Eur. J. Biochem.* **1976**, *67*, 295−302. (b) Zappelli, P.; Rossodivita, A.; Re, L. *Eur. J. Biochem.* **1975**, *54*, 475−482. (c) Bückmann, A. F. *Biocatalysis* **1987**, *1*, 173−186. (d) Leca, B.; Marty, J.-L. *Biosens. Bioelectron.* **1997**, *12*, 1083−1088. (e) Leca, B.; Marty, J.-L. *Anal. Chim. Acta* **1997**, *340*, 143−148. (f) Nakamura, A.; Urabe, I.; Okada, H. *J. Biol. Chem.* **1986**, *261*, 16792−16794.
(19) (a) Mansson, M.-O.; Larsson, P.-O.; Mosbach, K. *Eur. J. Biochem.* **1978**, *86*, 455−463. (b) Mansson, M.-O.; Larsson, P.-O.; Mosbach, K. *FEBS Lett.* **1979**, *98*, 309−313. (c) Goulas, P. *Eur. J. Biochem.* **1987**, *168*, 469−473.
(20) Furukawa, S.; Katayama, N.; Iizuka, T.; Urabe, I.; Okada, H. *FEBS Lett.* **1980**, *121*, 239−242.
(21) Leca, B.; Marty, J.-L. *Biosens. Bioelectron.* **1997**, *12*, 1083−1088.
(22) (a) Bardea, A.; Katz, E.; Bückmann, A. F.; Willner, I. *J. Am. Chem. Soc.* **1997**, *119*, 9114−9119. (b) Katz, E.; Heleg-Shabtai, V.; Bardea, A.; Willner, I.; Rau, H. K.; Haehnel, W. *Biosens. Bioelectron.* **1998**, *13*, 741−756.
(23) (a) Bückmann, A. F.; Wray, V.; Stocker, A. In *Methods in Enzymology: Vitamins and Coenzymes*; McCormick, D. B., Ed.; Academic Press: Orlando, FL, 1997; Vol. 280, Part 1, p 360. (b) Bückmann, A. F.; Wray, V. *Biotechnol. Appl. Biochem.* **1992**, *15*, 303−310.
(24) Zayats, M.; Katz, E.; Willner, I. *J. Am. Chem. Soc.* **2002**, *124*, 2120−2121.
(25) Morris, D. L.; Buckler, R. T. In *Methods in Enzymology*; Langone, J. J., Van Vunakis, H., Eds.; Academic Press: Orlando, FL, 1983; Vol. 92, Part E, pp 413−417.

Scheme 1. Covalent Coupling of FAD Cofactor to a Phenylboronic Acid-Functionalized Au-Electrode: (Route a) Formation of a Mixed FAD/Long Chain Thiol Rigidified Monolayer; (Route b) Reconstitution of Apo-GOx on an FAD-Functionalized Electrode

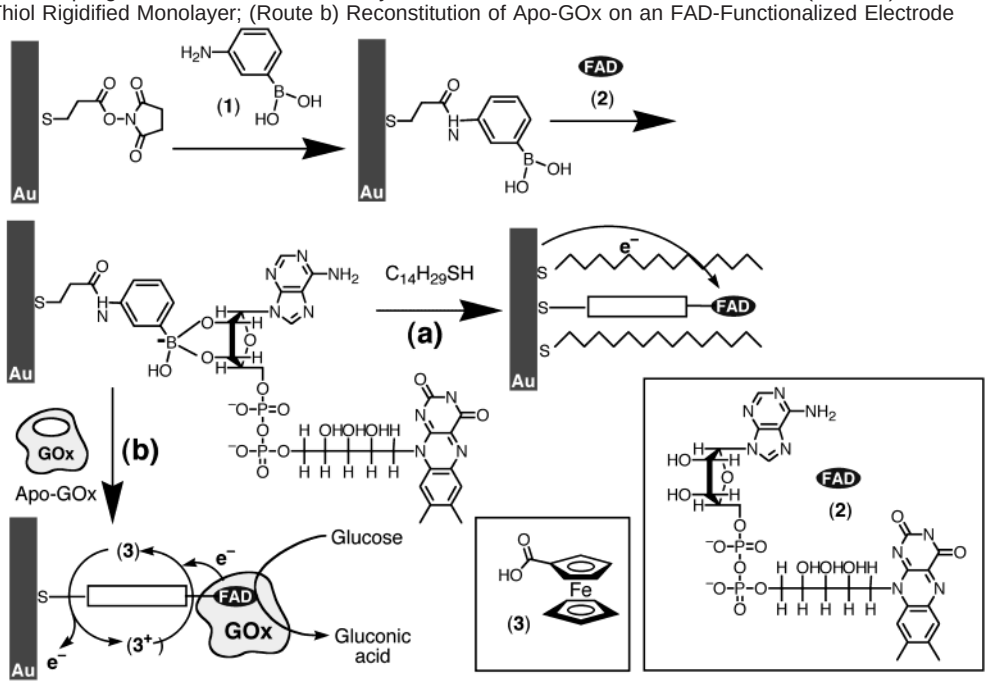

stored in concentrated sulfuric acid. Prior to the modification, the electrodes were rinsed with water, soaked for 10 min in concentrated nitric acid, and rinsed again with water. A cyclic voltammogram recorded in 1 M H_2SO_4 was used to determine the purity and roughness of the electrode surface just before modification.[26] The Au-electrodes were soaked in a solution of 0.05 M cystamine in water for 1 h and then rinsed thoroughly with water to remove the physically adsorbed cystamine. The cystamine-modified Au-electrodes were incubated for 2 h in a 3 mM solution of PQQ in 0.1 M HEPES-buffer, pH = 7.2, in the presence of 5 mM EDC. The PQQ-functionalized electrodes[27] were then reacted with 1 mM 3-aminophenylboronic acid solution in 0.1 M HEPES-buffer, pH = 7.2, in the presence of 5 mM EDC for 2 h. The electrodes were then rinsed with water to remove the physically adsorbed material. The Au-electrodes functionalized with PQQ and the covalently bound phenylboronic ligand were used for further functionalization with NAD^+, $NADP^+$, or FAD cofactors. The functionalized Au-electrodes were reacted with 1 mM of the respective cofactor solution in 0.1 M phosphate buffer, pH = 7.0, for 2 h, and then washed with water. This resulted in the Au-electrodes functionalized with PQQ redox-relay and the respective cofactor unit (NAD^+, $NADP^+$, or FAD) covalently bound to the monolayer interface via phenylboronic acid ligand units. The PQQ-FAD-functionalized Au-electrodes were reacted with 1 mg mL^{-1} apo-GOx in 0.1 M phosphate buffer, pH = 7.0, for 5 h (unless stated differently) at room temperature. The Au-electrodes were washed with water to yield the GOx-reconstituted electrodes for biocatalytic oxidation of glucose. The PQQ-NAD^+- and PQQ-$NADP^+$-functionalized Au-electrodes were reacted with 1 mg mL^{-1} LDH and 1 mg mL^{-1} MalD, respectively, in 0.1 M phosphate buffer, pH = 7.0, for 20 min at room temperature, briefly washed with water, and then reacted with 10% (v/v) glutaric dialdehyde in 0.1 M phosphate buffer, pH = 7.0, for 20 min. The resulting Au-electrodes were washed with water to yield the cross-linked LDH-NAD^+-integrated electrodes for the biocatalytic oxidation of lactate and cross-linked MalD-$NADP^+$-integrated electrodes for the biocatalytic oxidation of malic acid, respectively. To characterize the binding mode of the FAD cofactor, Au-electrodes were functionalized with FAD units omitting PQQ relay groups. The Au-electrodes were reacted with 10 mM dithiobis(succinimidylpropionate) in dry dimethyl sulfoxide (DMSO) for 30 min, rinsed with DMSO, and then briefly rinsed with water. The active ester-functionalized Au-electrodes were reacted with 1 mM 3-aminophenylboronic acid solution in 0.1 M HEPES-buffer, pH = 7.2, for 2 h, washed with water, and then reacted with 1 mM FAD solution in 0.1 M phosphate buffer, pH = 7.0, for 2 h to generate Au-electrodes functionalized with FAD cofactor units covalently bound to the surface by the phenylboronic acid ligand. These electrodes were used for two kinds of experiments: (i) The FAD-functionalized Au-electrodes were reacted with 1 mg mL^{-1} apo-GOx in 0.1 M phosphate buffer, pH = 7.0, for 5 h to obtain GOx-reconstituted electrodes that lack the PQQ-relay units. (ii) The FAD-functionalized Au-electrodes were treated with 1 mM 1-tetradecanethiol ($C_{14}H_{29}SH$) in ethanol for 2 h to obtain a rigidified monolayer of the FAD cofactor with a stretched spacer.

Electrochemical Measurements. A conventional three-electrode cell, consisting of the enzyme-modified Au working electrode, a glassy carbon auxiliary electrode isolated by a glass frit, and a saturated calomel reference electrode (SCE) connected to the working volume with a Luggin capillary, was used for the electrochemical measurements. All potentials are reported with respect to the SCE. Argon bubbling was used to remove oxygen from the solutions in the electrochemical cell, unless otherwise stated. The cell was placed in a grounded Faraday cage. Cyclic voltammetry, chronoamperometry, and impedance measurements were performed using an electrochemical analyzer composed of a potentiostat/galvanostat (EG&G model 283) and frequency response detector (EG&G model 1025) connected to a computer (EG&G software no. 270/250 and PowerSuite 2.11.1 for cyclic voltammetry/chronoamperometry and impedance spectroscopy, respectively). Faradaic impedance measurements were performed in the frequency range of 100 mHz to 10 kHz. The impedance spectra were plotted in the form of complex plane diagrams (Nyquists plots). The experimental impedance spectra were fitted to a theoretical equivalent circuit using commercial software (Zview, version 2.1b, Scribner Associates, Inc.). A Au rotating disk electrode (RDE) (geometrical area 0.16 cm^2, roughness factor ca. 1.2) was polished with an alumina suspension (0.3 μm, Buehler, IL), rinsed with water, and then modified with PQQ-FAD and reconstituted GOx as described above for the Au wire electrodes. The rotating disk electrode (RDE) measurements were

(26) Woods, R. In *Electroanalytical Chemistry*; Bard, A. J., Ed.; Marcel Dekker: New York, 1980; p 1.
(27) Katz, E.; Schlereth, D. D.; Schmidt, H.-L. *J. Electroanal. Chem.* **1994**, *367*, 59−70.

performed with an electrode rotator (model 636, EG&G). The rate of rotation was increased stepwise, and after each step the anodic current was measured when it had stabilized (after a few seconds).

Microgravimetric Measurements. A QCM analyzer (Fluke 164T multifunction counter, 1.3 GHz, TCXO) linked to a computer with a homemade software was used for microgravimetric measurements. Quartz-crystals (AT-cut, ca. 9 MHz, EG&G) sandwiched between two Au-electrodes (geometrical area 0.2 cm^2, roughness factor ca. 3.5) were used. The Au-electrode surfaces were washed with ethanol and modified in the same way as described above for the Au wire electrodes. Frequency changes of the quartz-crystals were measured in air after each modification step. All of the measurements were carried out at ambient temperature (22 ± 2 °C).

Results and Discussion

Alkyl or aryl boronic acids form boronate complexes with vicinal diols and specifically diols in rigidified *cis*-configurations. A flavin adenine dinucleotide (FAD) monolayer was linked to a Au-surface as outlined in Scheme 1.

A *N*-hydroxy-succinimide active ester monolayer was assembled on a Au-electrode. 3-Aminophenylboronic acid (**1**) was reacted with the monolayer to yield the phenylboronic acid interface. The resulting monolayer was then interacted with FAD (**2**), to yield the FAD-boronate complex on the electrode support. Figure 1A, curves a and b, shows the cyclic voltammograms of the phenylboronic acid interface before and after the binding of FAD through the formation of the FAD-boronate complex, respectively. The FAD-monolayer reveals a quasi-reversible redox-wave (peak-to-peak separation $\Delta E = 50$ mV at 200 mV s^{-1}) at a formal potential $E^\circ = -0.49$ V (pH = 7.0). Coulometric assay of the redox-waves of the FAD units indicates a surface coverage, Γ_{FAD}, that corresponds to 1.7×10^{-10} mol cm^{-2}. The resulting FAD monolayer was then rigidified with 1-tetradecanethiol ($C_{14}H_{29}SH$) to yield a densely packed interface, Scheme 1, route a. The cyclic voltammogram of the FAD/$C_{14}H_{29}SH$-mixed monolayer, Figure 1A, curve c, shows the electrochemical response characteristic to the FAD units without alteration of the redox potential and the surface coverage, but with a significant decrease of a capacitance current typical for densely packed monolayers. This process was used to probe the binding mode(s) of the FAD unit to the phenylboronic acid interface. As the FAD contains the cyclic ribose unit, and the linear oligohydroxyl chain, two binding modes to yield the boronate complex are, in principle, possible. Previous studies have indicated that the interfacial electron-transfer rate constants to redox-active units associated with the electrode are sensitive to the structural orientation and alignment of the redox components with respect to the electrode.[28] It was demonstrated that redox components linked in a rigidified monolayer structure to the electrode by two different binding modes reveal biexponential interfacial electron-transfer kinetics with different electron-transfer rate constants to the redox units in the two binding modes. Thus, the linkage of the FAD to the electrode in the form of two different boronate complexes is anticipated to yield a biexponential electron transfer rate between the redox unit and the electrode. Figure 1B shows the chronoamperometric current transient upon the application of a potential step from −0.4 to −0.6 V on the rigidified FAD-boronate monolayer associated with the Au-electrode. The current transient, corresponding to the reduction of FAD, reveals a monoexponential

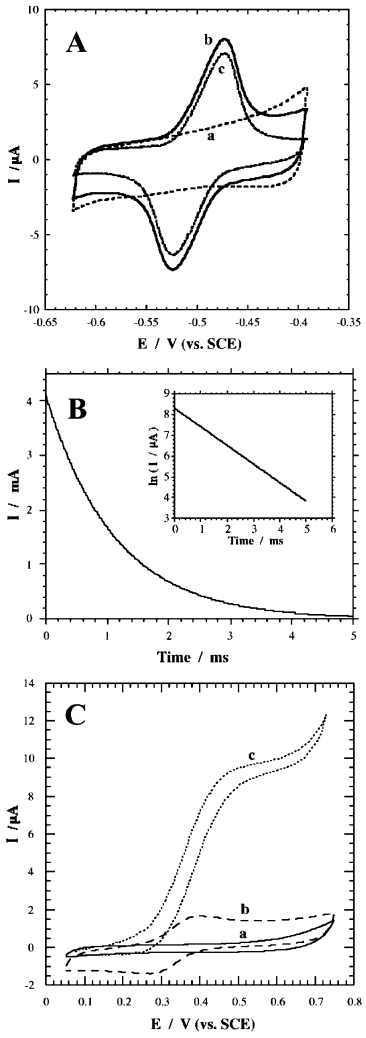

Figure 1. Electrochemical characterization of a FAD-phenylboronic acid-functionalized Au-electrode. (A) Cyclic voltammograms of a Au-electrode modified with the following: (a) 3-Aminophenylboronic acid covalently linked to a cysteic acid monolayer. (b) Covalently linked FAD to the 3-aminophenylboronic acid layer. (c) The FAD-monolayer rigidified with $C_{14}H_{29}SH$ thiol. Potential scan rate 200 mV s^{-1}. (B) Chronoamperometric current transient resulting from the application of a potential step from −0.4 to −0.6 V on the phenylboronic acid-FAD-rigidified monolayer-functionalized Au-electrode. Inset: The semilogarithmic plot of the current transient. (C) Cyclic voltammograms of GOx reconstituted on the phenylboronic-FAD-functionalized Au-electrode in the presence of the following: (a) 50 mM glucose, (b) 1 mM ferrocene monocarboxylic acid (**3**) in the absence of glucose, (c) 50 mM glucose and 1 mM ferrocene monocarboxylic acid (**3**). Potential scan rate 5 mV s^{-1}. The data were recorded in 0.1 M phosphate buffer, pH = 7.0, under Ar.

decay (cf. Figure 1B, inset), indicating a single-mode binding of FAD on the boronic acid interface. The interfacial electron-transfer rate constant was derived from eq 1,[28] where k_{et} is the interfacial electron-transfer rate constant, and Q_{FAD} is the charge associated with the reduction of the surface-confined FAD units. The surface coverage of the FAD units, Γ_{FAD}, can be found using eq 2, where A is the real electrode area, n is the number of electrons involved in the reduction process of a single FAD molecule, $n = 2$, and F is the Faraday constant.

$$I = k_{et} \cdot Q_{FAD} \exp(-k_{et} \cdot t) \quad (1)$$

$$\Gamma_{FAD} = Q_{FAD}/(n \cdot F \cdot A) \quad (2)$$

The interfacial electron-transfer rate constant corresponds to k_{et}

(28) Katz, E.; Willner, I. *Langmuir* **1997**, *13*, 3364−3373.

Scheme 2. Reconstitution of Apo-GOx on a PQQ-Phenylboronic Acid-FAD-Functionalized Au-Electrode

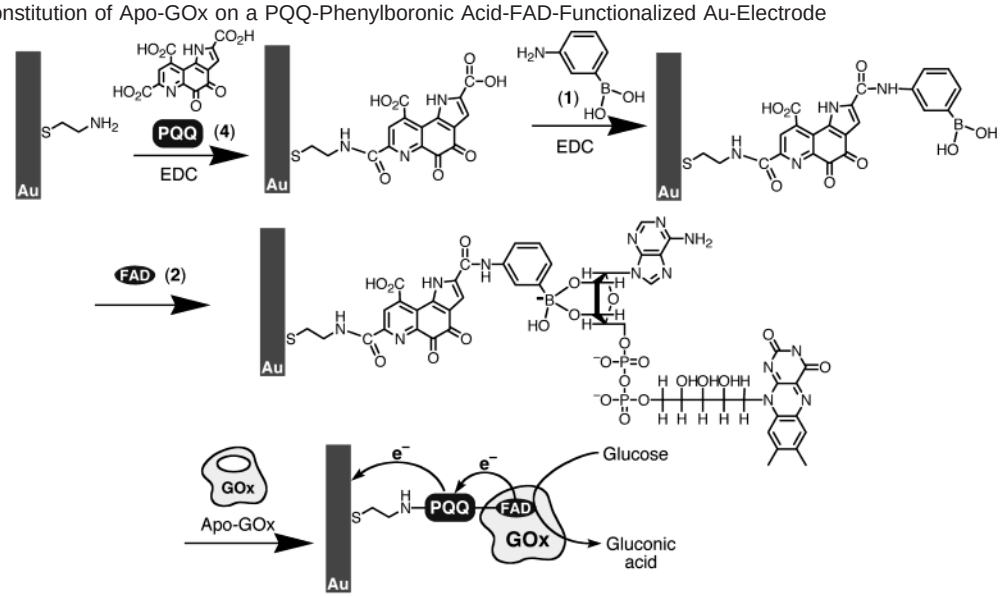

$= 900\ s^{-1}$, and the preexponential factor, $k_{et}{\cdot}Q_{FAD}$, is ca. 4.1 mA, which translates to a surface coverage of ca. 1.7×10^{-10} mol cm^{-2}, similar to the value derived by the coulometric analysis of the redox-wave of the FAD units. It is known from literature that boronate complexes with cyclic *cis*-diols reveal association constants that are larger by 2 orders of magnitude than those with linear vicinal diols.[29] Thus, the single mode of binding of FAD to the boronic acid monolayer can be attributed to the formation of the boronate complex with the ribose unit (vide infra).

The monolayer of the FAD-boronate complex was reacted with apo-glucose oxidase (apo-GOx) to yield the surface-reconstituted enzyme-electrode, Scheme 1, route b. Complementary microgravimetric quartz-crystal microbalance experiments revealed that the apo-GOx was reconstituted on the phenylboronic acid-FAD monolayer associated with a Au-quartz crystal. The surface coverage of the reconstituted enzyme was estimated to be 2.1×10^{-12} mol cm^{-2}. The resulting reconstituted enzyme-electrode is inactive toward the bioelectrocatalyzed oxidation of glucose, Figure 1C, curve a. The reconstituted enzyme exists, however, in a bioactive configuration on the electrode support, and addition of ferrocene carboxylic acid (**3**) as diffusional electron mediator activates the bioelectrocatalyzed oxidation of glucose, as reflected by the electrocatalytic anodic currents developed by the enzyme-electrode in the presence of glucose, Figure 1C, curve c.

To generate an integrated, electrically contacted, enzyme-electrode by the boronate-FAD reconstituted biocatalyst, we decided to reconstitute apo-GOx on a relay-FAD monolayer assembly, where the relay unit acts as mediator that facilitates electron transfer from the FAD site to the electrode. Scheme 2 depicts the stepwise assembly of the integrated enzyme-electrode. Pyrroloquinoline quinone, PQQ (**4**), was covalently linked to a cystamine monolayer assembled on a Au-electrode.[27] Covalent linkage of 3-aminophenylboronic acid (**1**) to the monolayer, followed by the formation of the boronate-FAD complex, yields the relay-FAD interface. Apo-glucose oxidase was then reconstituted on the latter interface to yield the enzyme-electrode.

Figure 2, curve a, shows the cyclic voltammogram of the PQQ-monolayer-functionalized electrode. A quasi-reversible redox-wave at $E^\circ = -0.13$ V (pH = 7.0) is observed. Coulometric assay of the reduction (or oxidation) wave of PQQ, and taking into account a two-electron redox-process,[27] indicates

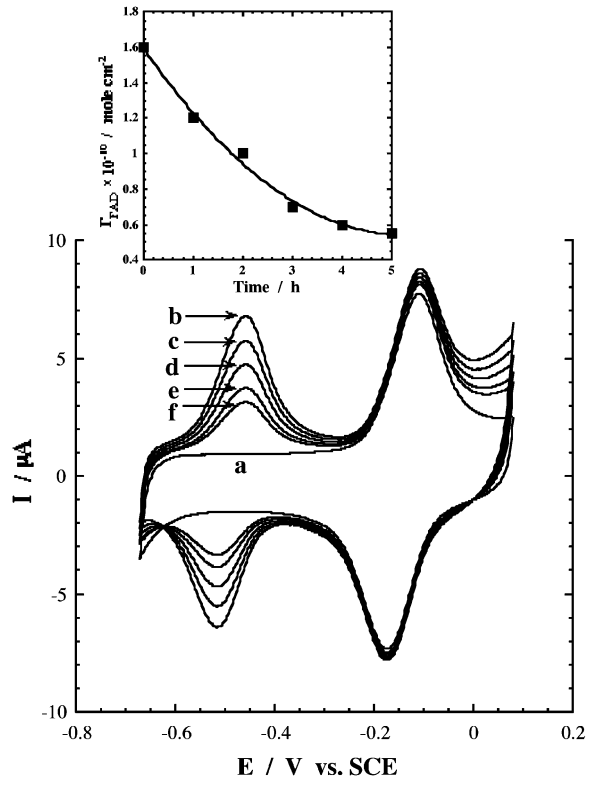

Figure 2. Cyclic voltammograms of the PQQ-phenylboronic acid-FAD-functionalized Au-electrode upon its interaction with apo-GOx: (a) PQQ-phenylboronic acid-functionalized Au-electrode prior to the binding of FAD cofactor. (b) PQQ-phenylboronic acid-FAD-functionalized Au-electrode prior to the interaction with apo-GOx. (c−f) The PQQ-phenylboronic acid-FAD-functionalized Au-electrode after 1, 2, 3, and 4 h of interaction with apo-GOx, respectively. The data were recorded in 0.1 M phosphate buffer, pH = 7.0, under Ar, potential scan rate 200 mV s^{-1}. Reconstitution was performed in the presence of 1 mg mL^{-1} apo-GOx at room temperature. Inset: The surface concentration of the electrochemically active FAD at time intervals of the reconstitution process. The Γ_{FAD} values were derived from the cathodic peaks of the respective cyclic voltammograms.

(29) Lorand, J. P.; Edwards, J. D. *J. Org. Chem.* **1959**, *24*, 769−774.

a surface coverage that corresponds to 1.8×10^{-10} mol cm^{-2}. Figure 2, curve b, shows the cyclic voltammogram of the FAD-PQQ-monolayer that reveals the redox waves at $E^\circ = -0.49$ V and $E^\circ = -0.13$ V (at pH = 7.0) for the FAD and PQQ units, respectively.

The surface coverage of the FAD units corresponds to 1.6×10^{-10} mol cm^{-2}. Thus, almost a quantitative formation of a PQQ-FAD dyad (PQQ:FAD = 1:0.9 molar ratio) was achieved upon binding of the secondary FAD units to the primary PQQ units assembled on the electrode surface. Interaction of the PQQ-FAD monolayer-modified electrode with apo-GOx results in the time-dependent depletion of the electrical response of the FAD sites, but the electrical response of the PQQ units is unaffected, Figure 2, curves b−f. The decrease in the electrical response of the FAD sites may be attributed to their reconstitution into the apo-enzyme, which leads to the electrical insulation of the cofactor sites. The unaffected electrical response of the PQQ units implies that the relay units are positioned at the exterior of the protein, or close to its surface periphery. Figure 2, inset, depicts the time-dependent decrease of the surface content of FAD units which communicate with the electrode, as a result of the surface reconstitution process. Evidently, ca. 63% of the original FAD sites (1.6×10^{-10} mol cm^{-2}) lose their electrochemical activity. Thus, ca. 1×10^{-10} mol cm^{-2} of the FAD sites are electrically insulated upon reconstitution.

Parallel microgravimetric quartz-crystal microbalance, QCM, analyses were performed, where the stepwise reconstitution of apo-glucose oxidase is performed on a Au-quartz crystal. We find that the surface coverages of the PQQ, phenylboronic acid ligand, and coupled FAD are 1.8×10^{-10}, 1.6×10^{-10}, and 1.6×10^{-10} mol cm^{-2}, respectively, very similar to the surface coverages derived from the electrochemical experiments. The surface reconstitution of the apo-GOx enzyme resulted in a frequency change of $\Delta f = 200$ Hz, which translates[30] to a surface coverage of 2×10^{-12} mol cm^{-2}. This surface coverage is characteristic of a densely packed monolayer of GOx. Assuming that a single GOx molecule has a footprint[31] of 58 nm^2, an ordered densely packed monolayer of the enzyme exhibits a surface coverage of 2.9×10^{-12} mol cm^{-2}, and this value translates to a surface coverage of 2.0×10^{-12} mol cm^{-2} for the random densely packed GOx monolayer (ca. 70% of the ordered packing).[32] Realizing that apo-GOx includes two subunits for the binding of the FAD cofactor, this surface coverage is ca. 25-fold lower than the surface coverage of the FAD sites that are insulated upon reconstitution of the apo-GOx. This may be attributed to the nonspecific incorporation of FAD sites into the protein, resulting in the blocking of their electrical communication with the electrode.

The surface-reconstitution of apo-GOx on the PQQ-FAD monolayer is further supported by Faradaic impedance spectroscopy measurements, Figure 3. The interfacial electron-transfer resistance, R_{et} (approximately the diameter of the semicircle domain in the Faradaic impedance spectra plotted as a Nyquist diagram),[33] increases upon binding of protein molecules to an electrode surface, which results in a barrier for

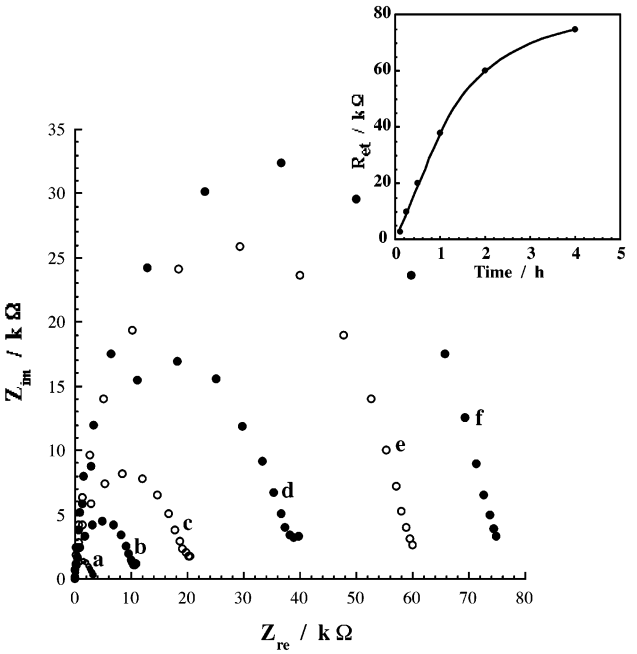

Figure 3. Faradaic impedance spectra (Nyquist plots) of the PQQ-phenylboronic acid-FAD-functionalized Au-electrode at time intervals of apo-GOx reconstitution (apo-GOx, 1 mg mL^{-1}): (a) 0.1 h, (b) 0.25 h, (c) 0.5 h, (d) 1 h, (e) 2 h, (f) 4 h. The data were recorded in 0.1 M phosphate buffer, pH = 7.0, in the presence of $[Fe(CN)_6]^{3-/4-}$ (1:1), 10 mM, biasing potential 0.17 V, at room temperature. Inset: The R_{et} values of the electrode as a function of the reconstitution time.

electron exchange between the conductive support and a solubilized redox probe.[34] The exact values of R_{et} were found by computer fitting of the experimental impedance spectra with an equivalent electronic circuit of Randles and Ershler type.[33,35] When the reconstitution of apo-GOx proceeds and the enzyme molecules bind to the FAD-modified electrode surface, the interfacial electron-transfer resistance, R_{et}, increases and then levels off as a result of saturation of the electrode by the reconstituted enzyme. From the time-dependent increase in the interfacial electron-transfer resistance, Figure 3, inset, the pseudo first-order reconstitution rate constant, $k_{reconst}'$, is estimated to be ca. 1 h^{-1}. However, it should be noted that the measured rate constant corresponds to the formation of the enzyme layer on the modified electrode surface, which does not necessarily mean it exists in a biocatalytically active state.

Figure 4 shows the cyclic voltammograms corresponding to the bioelectrocatalytic currents of the reconstituted enzyme-electrode at a constant glucose concentration of 8×10^{-2} M, at different times of reconstitution. It can be seen that as the reconstitution time is longer, the bioelectrocatalytic anodic current is enhanced, and it levels off and reaches a saturation value after ca. 5 h, the optimal time for the saturation of the surface with the reconstituted GOx. Figure 4, inset, shows the electrocatalytic anodic currents at $E = 0.2$ V at variable times of reconstitution. This curve represents the kinetics of reconstitution, and the derived pseudo first-order rate constant, $k_{reconst}''$

(30) Buttry, D. A.; Ward, M. D. *Chem. Rev.* **1992**, *92*, 1355−1379.
(31) Nakamura, S.; Hayashi, S.; Koga, K. *Biochim. Biophys. Acta* **1976**, *445*, 294−308.
(32) (a) Bourdillon, C.; Demaille, C.; Gueris, J.; Moiroux, J.; Savéant, J. M. *J. Am. Chem. Soc.* **1993**, *115*, 12264−12269. (b) Weibel, M. K.; Bright, H. J. *J. Biol. Chem.* **1971**, *246*, 2734−2744.
(33) (a) Bard, A. J.; Faulkner, L. R. *Electrochemical Methods: Fundamentals and Applications*; Wiley: New York, 1980. (b) Stoynov, Z. B.; Grafov, B. M.; Savova-Stoynova, B. S.; Elkin, V. V. *Electrochemical Impedance*; Nauka: Moscow, 1991.
(34) (a) Katz, E.; Alfonta, L.; Willner, I. *Sens. Actuators, B* **2001**, *76*, 134−141. (b) Alfonta, L.; Bardea, A.; Khersonsky, O.; Katz, E.; Willner, I. *Biosens. Bioelectron.* **2001**, *16*, 675−687.
(35) (a) Randles, J. E. B. *Discuss. Faraday Soc.* **1947**, *1*, 11−19. (b) Ershler, B. V. *Discuss. Faraday Soc.* **1947**, *1*, 269−277.

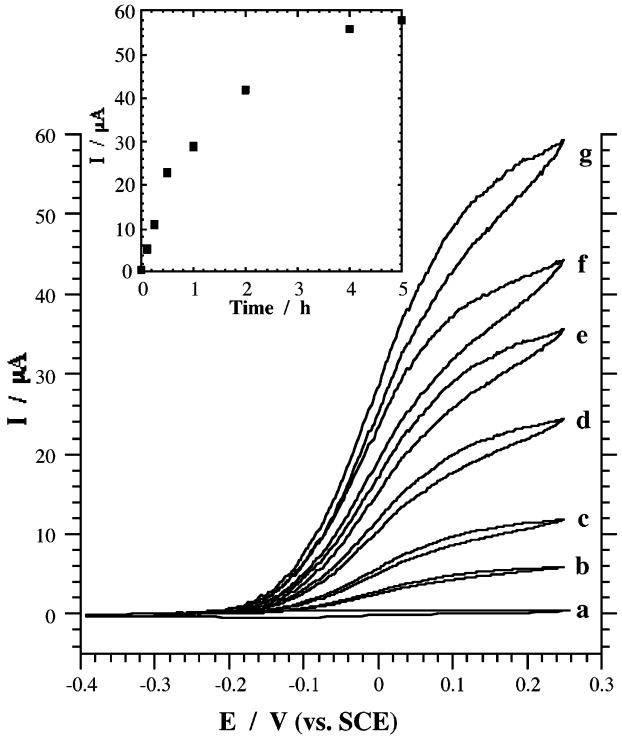

Figure 4. Cyclic voltammograms of the PQQ-phenylboronic acid-FAD-functionalized Au-electrode at variable time intervals of reconstitution with apo-GOx, 1 mg mL^{-1}: (a) 0 h, (b) 0.1 h, (c) 0.25 h, (d) 0.5 h, (e) 1 h, (f) 2 h, (g) 4 h. The data were recorded in 0.1 M phosphate buffer, pH = 7.0, in the presence of glucose, 80 mM, under Ar, at room temperature, potential scan rate 2 mV s^{-1}. Inset: The electrocatalytic currents produced by the electrode in the presence of glucose, 80 mM, at $E = 0.2$ V at variable time intervals of the reconstitution (derived from the respective cyclic voltammograms).

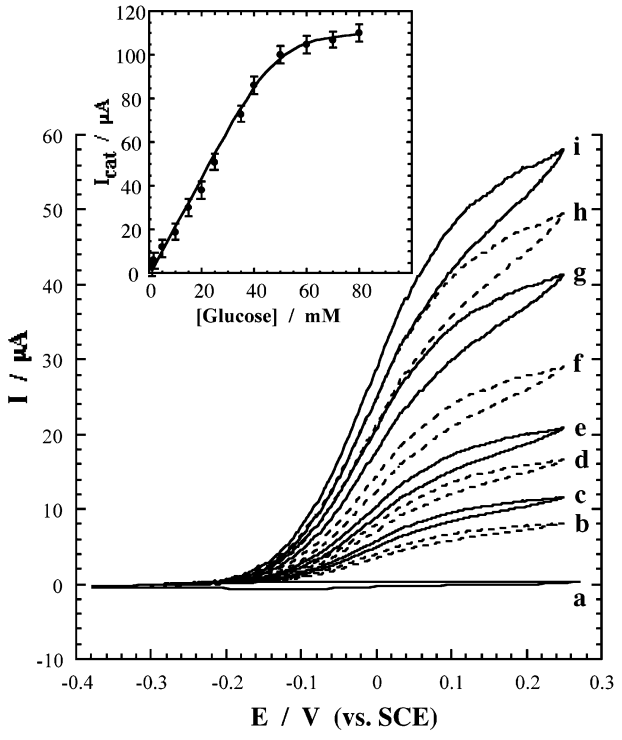

Figure 5. Cyclic voltammograms of the PQQ-phenylboronic acid-FAD-functionalized Au-electrode reconstituted with apo-GOx, 1 mg mL^{-1}, 5 h, in the presence of different concentrations of glucose: (a) 0 mM, (b) 5 mM, (c) 10 mM, (d) 15 mM, (e) 20 mM, (f) 25 mM, (g) 35 mM, (h) 40 mM, (i) 50 mM. The measurements were performed in 0.1 M phosphate buffer, pH = 7.0, under Ar, potential scan rate 2 mV s^{-1}. Inset: The calibration curve measured at $E = 0.2$ V.

$= 1\ h^{-1}$, coincides nicely with that, $k_{reconst}'$, obtained from the impedance spectroscopy results. It should be noted that the present rate constant corresponds to the increase of the biocatalytic activity of the electrode upon building up the layer of the reconstituted enzyme. Thus, it can be concluded that both rate constants, $k_{reconst}'$ and $k_{reconst}''$, the first reflecting the formation of the enzyme layer on the electrode, and the second reflecting the increase of the biocatalytic activity of the enzyme associated with the electrode, correspond to the same process of the enzyme reconstitution in its biocatalytic form.

Figure 5 shows the cyclic voltammograms of the reconstituted enzyme-electrode at different concentrations of glucose (a saturated GOx monolayer was generated upon 5 h of the reconstitution process). The electrocatalytic anodic currents indicate the effective bioelectrocatalyzed oxidation of glucose. As the electrocatalytic anodic current begins at $E = -0.13$ V, the redox potential of the PQQ units, we conclude that PQQ mediates the electron transfer between the FAD redox center of the reconstituted enzyme and the electrode. The electrocatalytic anodic currents increase as the concentration of glucose is elevated, and they level off at a glucose concentration that corresponds to ca. 6×10^{-2} M, Figure 5, inset.

Taking into account the saturated electrocatalytic current, $I_{cat}^{sat} = 110\ \mu$A, and knowing the real electrode area, $A = 0.4\ cm^2$, the surface coverage of the reconstituted enzyme, $\Gamma_{GOx} = 2 \times 10^{-12}$ mol cm^{-2}, and the number of electrons obtained upon oxidation of one glucose molecule, $n = 2$, we estimate using eq 3 the maximum turnover rate, TR_{max}, of the enzyme to be ca. 700 s^{-1} (molecules of glucose oxidized by one GOx molecule per second). The obtained TR_{max} value is similar to that of a natural glucose oxidase with its native O_2 electron acceptor.[36]

$$TR_{max} = I_{cat}^{sat}/(F \cdot n \cdot \Gamma_{GOx} \cdot A) \qquad (3)$$

Further characterization of the kinetics of the bioelectrocatalyzed oxidation of glucose by the reconstituted GOx-monolayer-electrode was accomplished by rotating disk electrode, RDE, experiments (see Supporting Information, Figure S1, and the respective discussion).

The reconstituted GOx-electrodes show a ca. 7% decrease in their electrical responses upon continuous operation for 24 h at room temperature (22 ± 2 °C). The GOx-electrodes are stable upon their storage in dry state under argon at 4 °C, and no noticeable degradation of the electrodes was observed upon their storage for 2 months.

The possibility of linking cofactor units to a phenylboronate ligand associated with a Au-electrode is not limited to the FAD cofactor. Other cofactors such as the nicotinamide cofactors, β-nicotinamide adenine dinucleotide (NAD^+), and β-nicotinamide adenine dinucleotide phosphate ($NADP^+$) include ribose units and hence could be linked to the boronate ligand. Thus, this binding motif may be useful for the design of integrated enzyme-electrodes that include $NAD(P)^+$-dependent enzymes. The development of integrated $NAD(P)^+$-dependent enzyme-electrodes is of substantial interest for tailoring of biosensors

(36) Eisenwiener, H. G.; Schultz, G. V. *Naturwissenschaften* **1969**, *56*, 563−564.

Scheme 3. Assembly of a Cross-Linked-Integrated Malate Dehydrogenase (MalD) Electrode on a PQQ-Phenylboronic Acid-NADP$^+$-Functionalized Surface

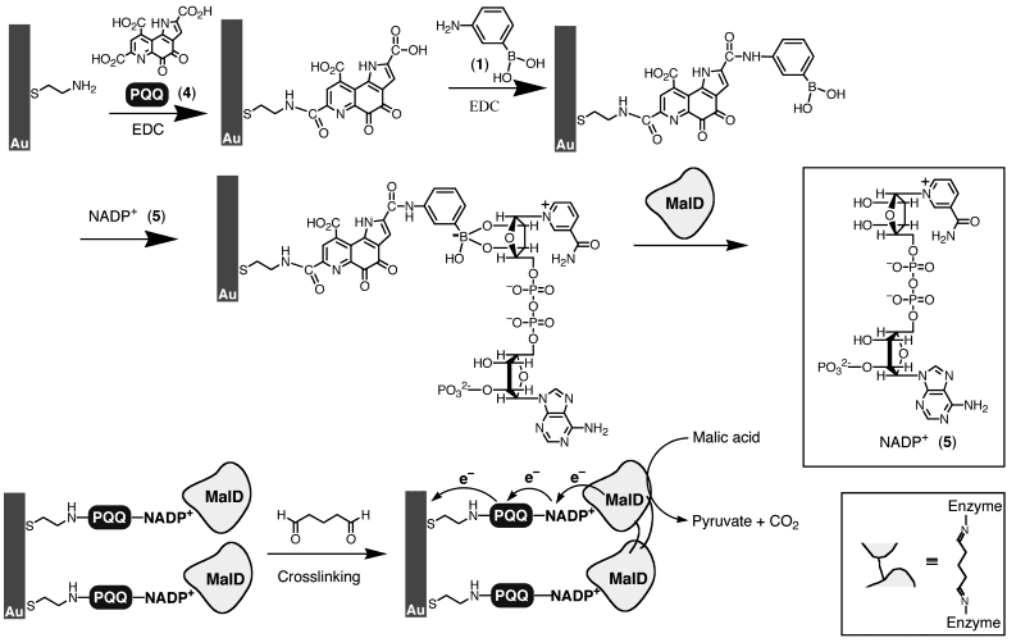

or biofuel cells, and is accompanied by severe limitations. In contrast to the FAD cofactor that is fixed to the protein, the NAD(P)$^+$ cofactors act diffusionally, and their confinement to the protein assembly is needed.[3] Furthermore, the NAD(P)$^+$ does not exhibit direct reversible electrochemistry. The two-electron electrochemical oxidation of the reduced 1,4-dihydronicotinamide cofactor, NADH or NADPH, generated upon the biocatalyzed oxidation of the respective substrates, is accompanied by high overpotentials. Different molecular catalysts were reported to catalyze the two-electron oxidation of NAD(P)H to NAD(P)$^+$.[12−14] Pyrroloquinoline quinone, PQQ, acts as an electrocatalyst for the two-electron oxidation of NAD(P)H,[15,16] and the electrocatalytic process is particularly efficient in the presence of Ca^{2+}-ions as cocatalyst.[15] These properties of PQQ were utilized to construct integrated NAD$^+$-dependent enzyme-electrodes.[22] The synthetic N^6-aminoethyl-β-nicotinamide adenine dinucleotide was covalently linked to a PQQ monolayer associated with a Au-electrode. The affinity complexes generated between the NAD$^+$-dependent enzymes lactate dehydrogenase or alcohol dehydrogenase[37] were cross-linked on the electrode supports to yield integrated electrically contacted enzyme-electrodes.[22] This concept was broadened by the use of native NAD(P)$^+$ cofactors and the phenylboronic acid as a bridging unit. β-Nicotinamide adenine dinucleotide phosphate (NADP$^+$, **5**) includes a single ribose unit for its association to the boronic acid ligand (a phosphate group restricts such reaction for the second ribose unit). Scheme 3 shows the assembly of an integrated electrode consisting of the NADP$^+$-dependent malate dehydrogenase.

A pyrroloquinoline quinone, PQQ, monolayer is assembled on the Au-electrode, surface coverage of 1.9×10^{-10} mol cm^{-2}. 3-Aminophenylboronic acid is covalently linked to the surface, and the resulting phenylboronic acid surface is reacted with NADP$^+$ to yield the phenylboronate-NADP$^+$ complex on the surface. Microgravimetric quartz-crystal microbalance measurements indicate that the coverage of the phenylboronic acid ligand monolayer and of the associated NADP$^+$ cofactor layer is 1.4×10^{-10} and 1.3×10^{-10} mol cm^{-2}, respectively (PQQ:NADP$^+$ = 1.4:1 − molar ratio). The resulting NADP$^+$-monolayer is then interacted with the malate dehydrogenase, MalD, to generate an affinity complex between MalD and the NADP$^+$ cofactor, and subsequently cross-linked with glutaric dialdehyde to generate an integrated two-dimensional enzyme layer. QCM measurements indicate that the surface coverage of the MalD is 1.2×10^{-12} mol cm^{-2}. The theoretical coverage of a random densely packed MalD monolayer is ca. 1.3×10^{-12} mol cm^{-2}, assuming an enzyme footprint of ca. 1×10^{-12} cm^{-2} per molecule[38] and taking into account ca. 70% filling in the random densely packed layer configuration.

Figure 6 shows the cyclic voltammograms corresponding to the bioelectrocatalyzed oxidation of malic acid in the presence of the PQQ-NADP$^+$-MalD-integrated enzyme-electrode. A bioelectrocatalytic anodic current begins at the redox potential of the PQQ electron-relay. The anodic currents increase as the concentration of malic acid is elevated. Control experiments reveal that neither the PQQ-monolayer electrode nor the PQQ-NADP$^+$ monolayer-electrode is active toward the electrocatalyzed oxidation of malic acid. Figure 6, inset, shows the calibration curve which corresponds to the electrocatalytic currents (derived from the respective cyclic voltammograms at $E = 0.2$ V) at different concentrations of malic acid. The anodic current levels off at a malate concentration of ca. 8×10^{-3} M. Using the saturated value of the anodic current, and the surface coverage of MalD, $\Gamma_{MalD} = 1.2 \times 10^{-12}$ mol cm^{-2}, we estimate the maximum turnover rate of the enzyme in the integrated electrode assembly to be 190 s^{-1} (molecules of malic acid oxidized by one MalD molecule per second). This value is substantially lower than the maximum turnover rate of the native

(37) Kharitonov, A. B.; Alfonta, L.; Katz, E.; Willner, I. *J. Electroanal. Chem.* **2000**, *487*, 133−141.

(38) The molecular dimensions of the respective proteins were estimated using commercial software HyperChem (Release 2) for Windows. The protein structures were taken from the Protein Data Bank (Brookhaven National Laboratory, http://www.rcsb.org/pdb). The error in the calculated dimensions of the proteins is estimated to be ±5 Å.

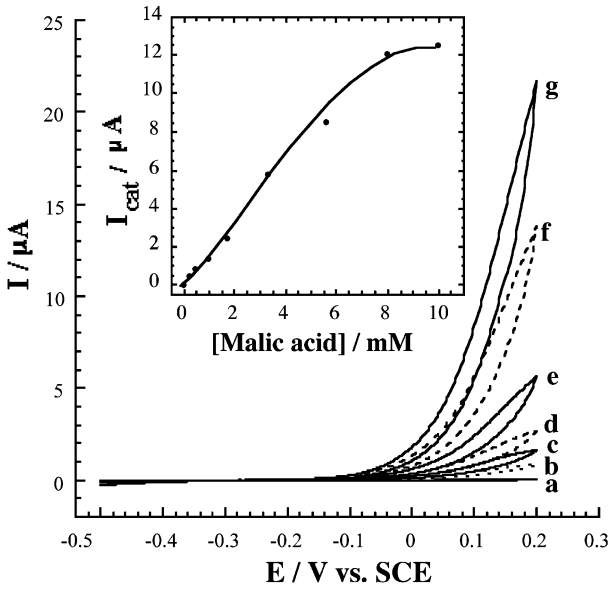

Figure 6. Cyclic voltammograms of the integrated enzyme-electrode obtained by cross-linking of malate dehydrogenase (MalD) associated with the PQQ-phenylboronic acid-$NADP^+$-functionalized electrode in the presence of different concentrations of malic acid: (a) 0 mM, (b) 0.25 mM, (c) 0.5 mM, (d) 1 mM, (e) 1.7 mM, (f) 3.3 mM, (g) 5.6 mM. The data were recorded in 0.1 M Tris-buffer, pH 7.0, with 10 mM $CaCl_2$, under Ar, at room temperature, potential scan rate 5 mV s^{-1}. Inset: The calibration curve of the electrocatalytic currents measured at $E = 0.2$ V.

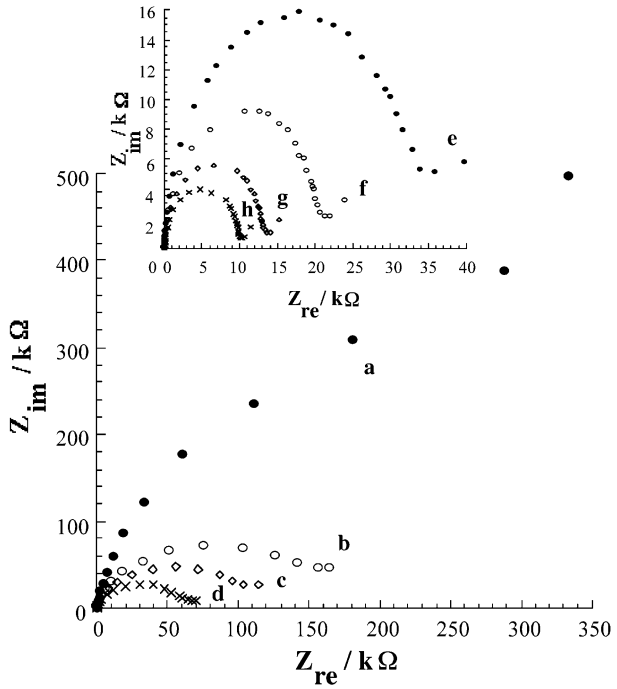

Figure 7. Faradaic impedance spectra (Nyquist plots) of the integrated enzyme-electrode obtained by cross-linking of malate dehydrogenase (MalD) associated with the PQQ-phenylboronic acid-$NADP^+$-functionalized electrode in the presence of different concentrations of malic acid: (a) 0 mM, (b) 0.25 mM, (c) 0.5 mM, (d) 1 mM, (e) 1.7 mM, (f) 3.3 mM, (g) 5.6 mM, (h) 8.0 mM. Note the different scales in the main part of the graph and in the inset. The data were recorded in 0.1 M Tris-buffer, pH 7.0, with 10 mM $CaCl_2$, under Ar, at room temperature, biasing potential $E = 0.25$ V.

enzyme with diffusional $NADP^+$, 5×10^3 s^{-1}.[39] The Michaelis−Menten constant, $K_M = 1 \times 10^{-2}$ M, was calculated from the calibration plot using the Lineweaver−Burke procedure,[40] and this value is significantly higher than the Michaelis−Menten constant of the native enzyme, $K_{M(native)} = 3.9 \times 10^{-4}$ M.[41] Several reasons may cause the lower turnover rate and the higher Michaelis−Menten constant for the enzyme in the integrated PQQ-$NADP^+$-MalD electrode: (i) The $NADP^+$ cofactor is in a rigidified configuration in the integrated assembly, which prohibits the free diffusion of the cofactor to the enzyme redox center where electron transfer proceeds. (ii) The generated NADPH is locked in the integrated assembly in a rigid configuration where its oxidation by the PQQ units is kinetically disfavored.

The bioelectrocatalytic oxidation of malic acid was characterized by impedance measurements. Faradaic impedance spectroscopy is often used for the characterization of biomaterial-modified electrodes, particularly in immunosensing or DNA sensing, by following the isolation of an electrode surface upon deposition of the respective biomolecules.[34] In this type of experiment, a layer of redox-inactive biomolecules that associates to the electrode surface creates a barrier for an electrochemical reaction between an external solubilized redox probe and the electrode support. We have already discussed the application of this method to follow the reconstitution process of the apo-GOx on the PQQ-FAD-functionalized electrode (cf. Figure 3). Nonetheless, the primary application of Faradaic impedance spectroscopy is in the kinetic analysis of electrochemical reactions.[33] This method is rarely used in biosensors, although it might be a very powerful method for the characterization of amperometric enzyme biosensors. The impedance spectrum of a bioelectrocatalytically active enzyme-electrode allows the determination of the electron-transfer resistance, R_{et}, of the system. The electron-transfer resistance translates into the exchange current under equilibrium, I_0, eq 4, and then the respective heterogeneous electron-transfer rate constant, k_{et}, can be evaluated, taking into account the dependence of k_{et} on the applied potential, eq 5, where $R = 8.31$ J mol^{-1} K is the gas constant, $T = 298$ K is the temperature, $n = 2$ is the number of electrons involved in the oxidation of the substrate molecule, $F = 9.65 \times 10^4$ C $equiv^{-1}$ is the Faraday constant, I_0 is the exchange current under equilibrium, k_{et} is the heterogeneous electron-transfer rate constant, [S] is the substrate, malic acid, concentration, $\alpha \approx 0.5$ is the electron-transfer coefficient, and η is the overpotential applied to the electrode. Because the exchange current at equilibrium, I_0, is controlled by the substrate concentration (under the condition that the enzyme is not saturated by the substrate), the electron-transfer resistance of the electrode is controlled by the substrate concentration. Thus, by following R_{et} at different substrate concentrations, k_{et} can be derived. The later rate constant corresponds to the limiting step in the bioelectrocatalytic oxidation (or reduction) of the substrate.

$$R_{et} = (R \cdot T)/(n \cdot F \cdot I_0) \quad (4)$$

$$I_0 = n \cdot F \cdot A \cdot k_{et} \cdot [S] \exp[(-\alpha \cdot n \cdot F \cdot \eta)/(R \cdot T)] \quad (5)$$

Figure 7 shows the Faradaic impedance spectra of the integrated PQQ-$NADP^+$-MalD electrode in the presence of different concentrations of malic acid. Approximate values of

(39) Schrock, H. L.; Gennis, R. B. *Biochim. Biophys. Acta* **1980**, *616*, 10−21.
(40) Barman, T. E. *Enzyme Handbook*; Springer-Verlag: New York, 1985; Vol. 1, pp 6−9.
(41) Rutter, W. J.; Lardy, H. A. *J. Biol. Chem.* **1958**, *233*, 374−382.

Scheme 4. Assembly of a Cross-Linked-Integrated Lactate Dehydrogenase (LDH) Electrode on a PQQ-Phenylboronic Acid-NAD$^+$-Functionalized Surface

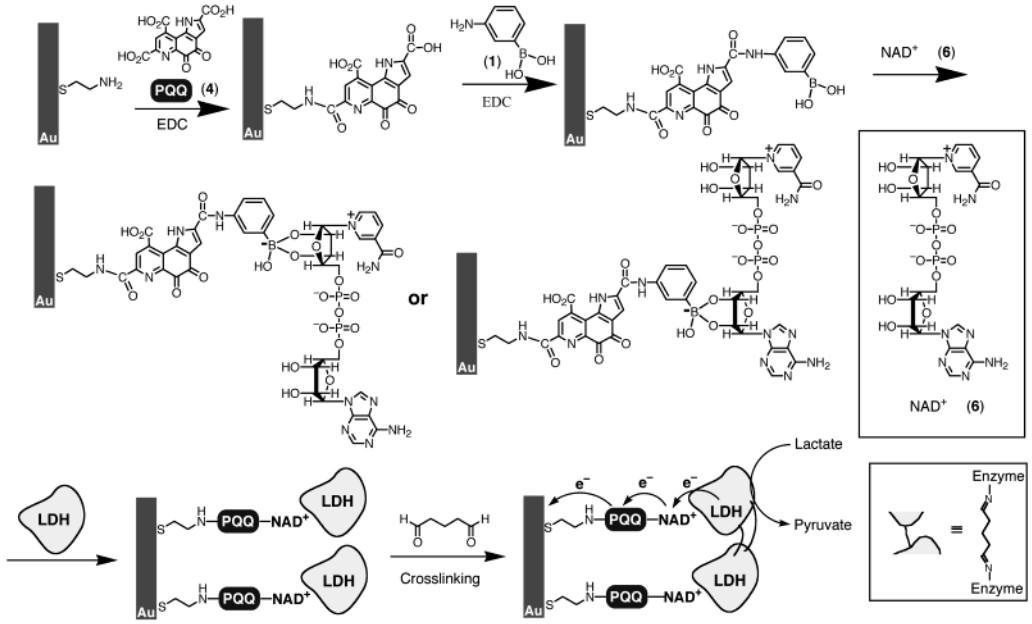

the electron-transfer resistance for each spectrum correspond to the diameters of semicircle domains of the respective spectra; however, precise numbers for R_{et} were obtained by computer fitting of the spectra to a theoretical equivalent circuit. The simplest equivalent circuit of the Randles and Ershler type[33,35] showed a good correlation with the experimental data, and therefore this model was used to find the R_{et} values from the experimental impedance spectra. Whereas the spectrum measured in the absence of malic acid (curve a) shows a very large electron-transfer resistance, $R_{et} > 1$ MΩ, the values of the electron-transfer resistance decrease upon increasing the malic acid concentration (curves b−h), reaching $R_{et} = 10$ kΩ at 8 mM of malic acid (note different scales in the main graph and the inset). The calibration plot of R_{et} at various concentrations of malic acid was derived from the impedance spectra (see Supporting Information, Figure S2). It should be noted that to obtain this calibration plot, much longer experiments were performed, and much more sophisticated electrochemical equipment was used than for the related amperometric measurements (cf. Figure 6). Therefore, this experiment was mainly performed for kinetic characterization of the biocatalytic system rather than for obtaining the calibration plot. Using eqs 4 and 5, assuming $\alpha \approx 0.5$, and taking into account that the spectra were recorded at $E = 0.25$ V ($\eta = 0.38$ V vs the potential of the terminal electron mediator PQQ), we found that $k_{et} \approx 2.56 \times 10^{-3}/([S] \cdot R_{et})$, where [S] is malic acid concentration (mol m^{-3}). We found from the experimental data that $[S] \cdot R_{et} \approx 6.8 \times 10^4$ mol m^{-3} Ω and that the electron-transfer rate constant $k_{et} \approx 3.8 \times 10^{-6}$ cm s^{-1}. It should be noted that the rate constant can be derived from a single impedance spectrum in the presence of the substrate (malic acid). The measurements of the impedance spectra with different concentrations of the malic acid are not necessary, and they were performed to demonstrate the possibility to follow the biocatalytic reaction with the Faradaic impedance spectroscopy and to find an average value of k_{et} at different substrate concentrations. Taking into account the surface coverage of MalD, $\Gamma_{MalD} = 1.15 \times 10^{-12}$ mol cm^{-2}, we calculated the overall rate constant that reflects the reaction of malic acid with the enzyme assembly, $k_{overall} = 8 \times 10^5$ M^{-1} s^{-1}.

Similarly, an attempt was made to fabricate an integrated, electrically contacted, electrode of the NAD$^+$-dependent enzyme lactate dehydrogenase, LDH, Scheme 4. In contrast to NADP$^+$, β-nicotinamide adenine dinucleotide (NAD$^+$, **6**) has two ribose units available for the reaction with the phenylboronic acid ligand, one close to the nicotinamide unit, similar to the NADP$^+$ cofactor, and a second ribose unit adjacent to the adenine component. Accordingly, two binding modes of the NAD$^+$ cofactor to the phenylboronic acid ligand are possible. Thus, 3-aminophenylboronic acid (**1**) was linked to the PQQ-functionalized electrode, and the resulting electrode was interacted with NAD$^+$, to yield the assemblies with the two different binding modes, Scheme 4. Microgravimetric QCM analyses indicate that the surface coverage of the PQQ units is ca. 1.9×10^{-10} mol cm^{-2} and the surface coverage of the NAD$^+$ units is ca. 2.0×10^{-10} mol cm^{-2} (PQQ:NAD$^+$ = 0.95:1 molar ratio). The generated NAD$^+$-modified electrode was interacted with lactate dehydrogenase, LDH, and the resulting cofactor-enzyme affinity complex[37] formed on the electrode was cross-linked with glutaric dialdehyde to yield the integrated relay-cofactor-enzyme-electrode. Quartz-crystal microbalance measurements indicate that the surface coverage of the cross-linked LDH is ca. 7.0×10^{-12} mol cm^{-2}.

Figure 8 shows the cyclic voltammograms observed upon the treatment of the integrated PQQ-NAD$^+$-LDH-electrode with different concentrations of lactate. An electrocatalytic anodic current starts at a potential characteristic to the redox potential of PQQ, $E° = -0.13$ V (pH = 7.0). The electrocatalytic current increases as the concentration of lactate is elevated. Figure 8, inset, shows the calibration curve that corresponds to the anodic current at $E = 0.2$ V at various concentrations of lactate. It can be seen that the electrocatalytic anodic current reaches a saturation value at a lactate concentration that corresponds to ca. 1.0×10^{-2} M. Control experiments reveal that no electro-

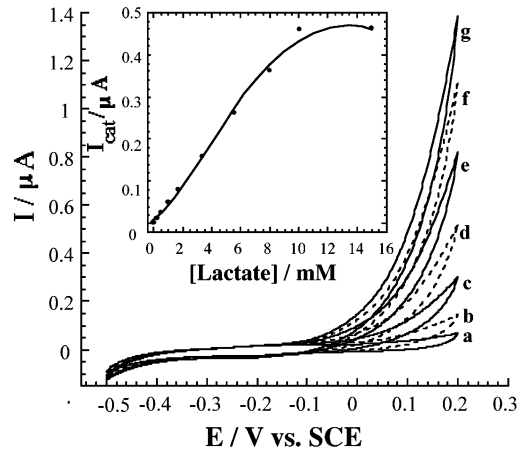

Figure 8. Cyclic voltammograms of the integrated enzyme-electrode obtained by cross-linking of lactate dehydrogenase (LDH) associated with the PQQ-phenylboronic acid-NAD^+-functionalized electrode in the presence of different concentrations of lactate: (a) 0 mM, (b) 0.5 mM, (c) 1.7 mM, (d) 3.3 mM, (e) 5.6 mM, (f) 8.0 mM, (g) 10.0 mM. The data were recorded in 0.1 M Tris-buffer, pH 7.0, with 10 mM $CaCl_2$, under Ar, at room temperature, potential scan rate 5 mV s^{-1}. Inset: The calibration curve of the electrocatalytic currents measured at $E = 0.2$ V.

catalytic anodic currents are observed in the absence of LDH. Also, the direct linkage of LDH to PQQ does not lead to any bioelectrocatalyzed oxidation of lactate. These results clearly indicate that the bioelectrocatalyzed oxidation of lactate by the integrated enzyme-electrode involves the biocatalyzed oxidation of lactate with the concomitant reduction of NAD^+ to NADH, followed by the PQQ-mediated electrocatalyzed oxidation of NADH, a process that regenerates the cofactor.[15,16] From the saturated electrocatalytic anodic current measured at $E = 0.2$ V ($I_{cat}^{saturated} = 0.45$ μA, cf. Figure 8, inset), and knowing the surface coverage of the enzyme, the maximum turnover rate of the enzyme is calculated to be 1.2 s^{-1} (molecules of lactate are oxidized by one enzyme molecule per second). This turnover rate of the enzyme in the integrated system is substantially lower than the turnover rate of the native LDH in solution, ca. 2300 s^{-1}.[42] Nonetheless, the observed turnover rate is very similar to that observed for another integrated LDH enzyme-electrode, where the affinity complex between LDH and a PQQ-amino-NAD^+ dyad is cross-linked on the electrode support.[22] Taking into account the value of the saturation current in the reported integrated system, and the surface coverage of the enzyme, we calculate a turnover rate of 2.5 s^{-1}. The low turnover rates of the enzyme in both integrated assemblies are attributed to the rigidity of the relay-cofactor-enzyme assembly. While the native process involves a diffusional route where NAD^+ penetrates the protein, is being reduced, and the reduced cofactor diffuses out of the protein, the integrated system on the electrode includes the cofactor in a structurally rigidified configuration. Electron transfer in these systems proceeds probably by a tunneling mechanism through intraprotein bonds.[43]

A further aspect that needs to be considered relates to the binding modes of the NAD^+ cofactor to the phenylboronic acid ligand. While $NADP^+$ includes only one ribose unit for the association to the boronic acid ligand, NAD^+ includes two ribose units, and hence two binding modes of the NAD^+ to the monolayer interface are feasible, Scheme 4. Thus, a fundamental question is whether the two binding modes are coexistent in the integrated enzyme-monolayer structure, and if both NAD^+ structures are present, do they differ in their electrical contacting features. Chronoamperometry proved to be an effective method to determine electron-transfer rates to (or from) redox units associated with monolayers on electrodes. It was also demonstrated that redox species differing in their spatial orientations relative to the electrode, or redox species linked to the electrode by tethers of different lengths, reveal different electron-transfer rate constants at the electrode interface.[28] The complexity of the present system originates from the fact that the $NAD(P)^+$ cofactors are not electrochemically active by themselves and their chronoamperometric responses upon potential steps cannot be directly measured as for FAD cofactor. However, the whole biocatalytic system, PQQ-$NADP^+$-MalD or PQQ-NAD^+-LDH in the presence of the respective substrates, malic acid or lactate, produces current upon application of a sufficiently positive potential to the electrode. The current formation includes the enzymatic reduction of $NAD(P)^+$ resulting in the formation of NAD(P)H that is further electrocatalytically oxidized by PQQ. The transient current responses of this system can be described by eq 6, where k_{et}' and k_{et}'' are the electron-transfer constants for two differently positioned $NA(P)D^+$/NAD(P)H cofactor units, and $Q_{NAD(P)H}'$ and $Q_{NAD(P)H}''$ are the charges associated with their oxidation upon the chronoamperometric experiment.

$$I = k_{et}' \cdot Q_{NAD(P)H}' \exp(-k_{et}' \cdot t) + k_{et}'' \cdot Q_{NAD(P)H}'' \exp(-k_{et}'' \cdot t) \quad (6)$$

The chronoamperometric experiment includes a potential step from the initial potential of -0.3 V where the biocatalytic current is blocked to the final potential of 0.2 V where a transient biocatalytic current appears. Accordingly, the transient bioelectrocatalytic anodic current developed by the PQQ-$NADP^+$-MalD-integrated electrode should reveal monoexponential kinetics due to a single binding mode of $NADP^+$, whereas the PQQ-NAD^+-LDH-integrated electrode could show a biexponential transient current, if both binding modes of the NAD^+ cofactor coexist, and if both of them provide significantly different electrochemical kinetics. Figure 9A shows the current transient observed for the integrated PQQ-boronic acid ligand-$NADP^+$-MalD electrode in the presence of malic acid upon the application of a potential step on the electrode from $E_{initial} = -0.3$ V to $E_{final} = 0.2$ V. Figure 9A, inset, shows the time-dependent current decay in a semilogarithmic plot. Clearly, the transient follows a single-exponential decay, $k_{et} = 14$ s^{-1}, as expected for a single-binding mode of $NADP^+$ to the surface. Figure 9B shows the current transient corresponding to the integrated PQQ-boronic acid NAD^+-LDH electrode in the presence of lactate upon the application of a potential step from $E_{initial} = -0.3$ V to $E_{final} = 0.2$ V. Figure 9B, inset, depicts the time-dependent current decay in a semilogarithmic plot. The current decay for this electrode reveals a biexponential decay, $k_{et}' = 1.3 \times 10^4$ s^{-1} and $k_{et}'' = 1.3 \times 10^3$ s^{-1}. From the preexponential factors, we derive that $Q_{NADH}':Q_{NADH}'' \approx 1:1$. Thus, the kinetic analysis of transient bioelectrocatalytic currents originating from the oxidation of lactate reveals that NAD^+ binds to the phenylboronic acid ligand by both of the possible ligation modes. One of the integrated systems formed by cross-

(42) Eichner, R. D. *Methods Enzymol.* **1982**, *89*, 359−362.
(43) (a) Gray, H. B.; Winkler, J. R. *J. Electroanal. Chem.* **1997**, *438*, 43−47. (b) Winkler, J. R.; Di Bilio, A. J.; Farrow, N. A.; Richards, J. H.; Gray, H. B. *Pure Appl. Chem.* **1999**, *71*, 1753−1764. (c) Tezcan, F. A.; Crane, B. R.; Winkler, J. R.; Gray, H. B. *Proc. Natl. Acad. Sci. U.S.A.* **2001**, *98*, 5002−5006.

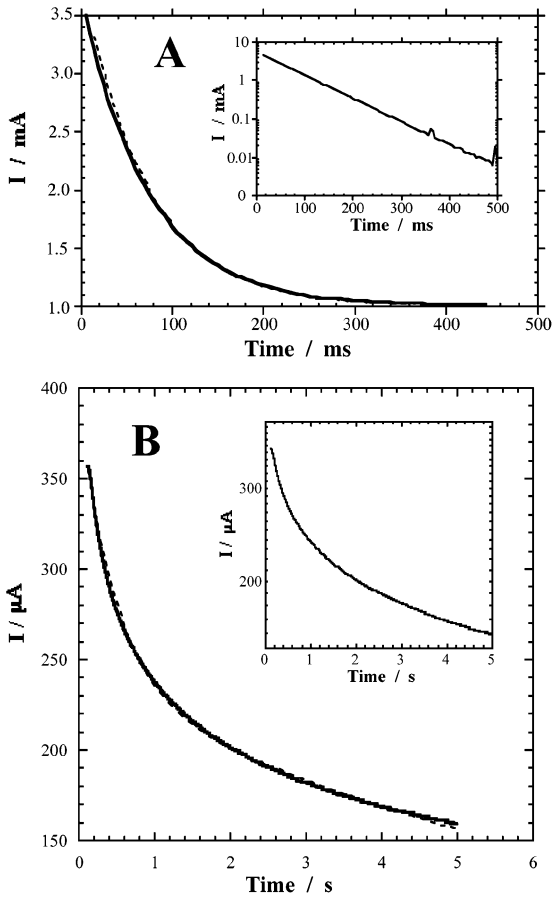

Figure 9. (A) Chronoamperometric current transient recorded for the integrated enzyme-electrode obtained by the cross-linking of malate dehydrogenase (MalD) associated with the PQQ-phenylboronic acid-NADP$^+$-functionalized electrode in the presence of malic acid, 10 mM, resulting from the application of a potential step from $E_{initial} = -0.3$ V to $E_{final} = 0.2$ V. Inset: The current transient in a semilogarithmic plot. (B) Chronoamperometric current transient recorded for the integrated enzyme-electrode obtained by the cross-linking of lactate dehydrogenase (LDH) associated with the PQQ-phenylboronic acid-NAD$^+$-functionalized electrode in the presence of lactate, 10 mM, resulting from the application of a potential step from $E_{initial} = -0.3$ V to $E_{final} = 0.2$ V. Inset: The current transient in a semilogarithmic plot. The data were recorded in 0.1 M Tris-buffer, pH 7.0, with 10 mM $CaCl_2$, under Ar, at room temperature.

linking of LDH to the two boronic acid-NAD$^+$ complexes is 10-fold more efficient than the second bioelectrocatalytic complex.

The integrated NAD$^+$/LDH and NADP$^+$/MalD electrodes reveal ca. 10% degradation in their activity upon continuous operation for 24 h at room temperature (22 ± 2 °C). The electrodes reveal, however, high stability upon their storage in the dry state under argon at 4 °C. Under these conditions, no observable degradation of the enzyme-electrodes was detected after storage for a period of 2 months.

Conclusions

The present study introduced a new method to construct electrically contacted enzyme-electrodes by using a phenylboronic acid ligand as the building block for the association of FAD or NAD(P)$^+$ cofactors. The surface-reconstitution of apo-flavoenzymes, for example, apo-glucose oxidase on the pyrroloquinoline quinone (PQQ)-phenylboronic acid-FAD monolayer, yields an aligned, electrically contacted, GOx electrode. Similarly, the cross-linking of affinity complexes generated between PQQ-phenylboronic acid-NAD(P)$^+$ interfaces and the biocatalysts MalD or LDH yields integrated electrically contacted NAD(P)$^+$-dependent enzyme-electrodes. While previous reports that addressed the generation of electrically contacted enzyme-electrodes of flavoenzymes by the reconstitution of the apo-proteins,[7] or of NAD(P)$^+$-dependent enzymes by the two-dimensional surface cross-linking of the proteins,[22] required the use of scarce synthetically modified cofactors, the present study reveals the direct coupling of the native cofactors to the surface. This new method turns the preparation of aligned flavoenzyme-electrodes or integrated NAD(P)$^+$-dependent enzyme-electrodes into an easy practice. The stability of the resulting electrodes, and particularly the integrated nature of the NAD(P)$^+$-dependent electrodes that does not reveal any leakage of the cofactors, suggest that such electrodes could be applied as biosensors or as active elements of biofuel cells.

Acknowledgment. This study is supported by the Israel-German Binational Program (DIP). M.Z. acknowledges the Levi Eshkol fellowship, the Israel Ministry of Science.

Supporting Information Available: Experimental details (PDF). This material is available free of charge via the Internet at http://pubs.acs.org.

JA027919Y